Performance of air and ground source heat pumps retrofitted to radiator heating systems and measures to reduce space heating temperatures in existing buildings

Manuel Lämmle, Constanze Bongs, Jeannette Wapler, Danny Günther, Stefan Hess[2], Michael Kropp[2], Sebastian Herkel

Fraunhofer Institute for Solar Energy Systems ISE, 79110 Freiburg, Germany
[2]INATECH - Albert-Ludwigs Universität Freiburg, 79108 Freiburg, Germany

Abstract

Heat pumps are expected to play a central role in decarbonizing heat supply, but face challenges in existing buildings due to high temperature requirements of existing radiator systems. This paper links the performance analysis of heat pump systems with methods to reduce temperatures of the space heating circuit. Field data and system simulations of air and ground source heat pumps show a linear correlation between the seasonal performance factor *SPF* and the mean heat pump temperature over a wide temperature range. Every Kelvin of reduced heat pump temperature increases the *SPF* by 0.10 – 0.13 points. Applied methods to reduce heating temperatures are demonstrated at existing multi-family buildings. Thermal insulation reduces the building's heat load, allowing a reduction of heating temperatures with the existing radiators. A further temperature reduction is achieved by analyzing the required heating power per room and identifying critical, undersized radiators. In a studied building, the selective exchange of only 7 % of all radiators is sufficient to reduce heating temperatures from 75°C/60°C to 55°C/45°C. This corresponds to a reduction of the electricity consumption by 40 – 42 %. However, the potential of these methods is specific for each building and depends particularly on its renovation state and installed radiator capacity. Nonetheless, an energy- and cost-efficient operation of heat pumps retrofitted in existing radiator heating systems is viable, if following the proposed system design method linking heat pump performance and reduction of space heating temperatures.

Keywords: building renovation; heat emission system; heat pump efficiency; building simulation; low exergy method

1. Introduction

Decarbonizing the heat supply of buildings is a core objective in the transition towards a low-carbon energy system [1]. Studies of future energy systems expect heat pumps to play a central role in supplying heat to residential and commercial buildings [2] and district heating networks [3], as they are considered an efficient power-to-heat technology utilizing low temperature ambient heat sources such as air or geothermal heat, and electricity from preferably renewable energy sources [4].

Heat pumps are an established technology in new buildings, where low temperature heating systems, such as radiant floor heating, leverage a high primary energy related efficiency. However, retrofitting heating systems with heat pumps remains a challenge in existing buildings [5]. High temperature requirements of conventional heating systems are one of the main technical obstacles to the diffusion of heat pumps in the building stock, particularly in multi-family buildings. Miara et al. [6] analyzed the seasonal performance of nearly 250 heat pump systems from field tests and found that heat pumps in existing buildings consume on average 20 % more electricity than heat pumps in new buildings. Huchtemann and Müller [7] evaluated field test data of retrofit heat pumps and identified the type of heat source and supply temperatures as decisive system parameters for an efficient operation.

The space heating emission system takes a central role in heat pump systems, as its heat transfer capability determines the required temperature levels. In this paper we focus on hydronic radiator heating systems as the predominant heat emission technology in existing buildings in Europe. Ovchinnikov et al. [8] reviewed hydronic space heating systems with regards to heat generation (district heating, heat pumps, boilers) and heat emission (conventional radiators, low temperature radiators, ventilation radiators, floor heating). Radiator heating systems are often oversized, e.g. due to large safety margins or previous energy-efficiency measures [9]. Oversized radiators leave a potential to be operated with reduced heating temperatures without compromising thermal comfort requirements [10]. Instead of exchanging the entire space heating system, it can be sufficient to selectively exchange only the bottleneck radiators which determine the maximum required system temperatures. Prerequisite for the application of these measures is hydronic balancing of the heat emission system with the purpose of ensuring an even flow distribution and thus low temperatures.

In the context of low temperature district heating networks, Østergaard and Svendsen [11] studied radiator heating systems in renovated buildings in Denmark for application of low temperature district heating. By identifying and selectively replacing four radiators in four buildings, they were able to reduce the nominal heating temperatures to 50°C/27°C, which corresponds to the nominal supply/return temperatures of the heating water at the design point. Jangsten et al. [9] carried out a survey on 109 radiator systems in a district heating network in Denmark and found that the studied buildings had varying return temperature levels between 42 °C and 88 °C. Therefore, every building must be analyzed individually with regards to its potential for reducing the supply and return temperatures. This potential is determined by the relationship of radiator capacity, building age, renovation state and nominal heating load.

For heat pump systems, Hasan et al. [12] combined radiator systems with radiant floor heating systems to achieve nominal supply and return temperatures of 45°C/35°C in existing Finnish apartment buildings. Sarbu and Sebarchievici [13] compared the energy

performance of a ground-coupled heat pump connected to a radiator and a radiant floor heating systems and concluded that radiator systems are sufficient for well-insulated buildings as nominal heating temperatures can be lowered to 55°C/45°C. Maivel and Kurnitski [14,15] studied the effect of low temperature heating systems on the heat distribution and emission losses in a detached Estonian building. The subsequent effect of low return temperatures improved the seasonal performance factor of an air source heat pump by 9 %. Wang et al. [16] compared conventional radiators at nominal temperatures of 75°C/50°C with a low-temperature radiator system at 45°C/35°C in combination with ventilation heat recovery. The average COP of an air source heat pump increased from 3.0 to 3.6 due to lower condenser temperatures.

The heat pump performance in multi-family buildings was studied by Fraga et al. [17] focusing on the availability and constraints of different heat sources. Heinz and Rieberer [18] carried out simulations for a propane-based air source heat pump in buildings with different renovation states and they analyzed the effect of renovation on heating curve temperatures and consequently seasonal performance factors. Nagy et al. [19] compared retrofit measures on the building envelope with an increase of heating surfaces by means of a thermal building model, which is calibrated from a small set of available data to identify cost-optimal strategies for zero-emission buildings. Calame et al. [20] compared the heating costs of air source, ground source and water-to-water heat pumps in retrofitted buildings and found that heating costs decrease in large multi-family buildings, where air source heat pumps can achieve similar heating costs as gas boilers.

Different control approaches to reduce temperatures in radiator heating systems were presented by Ionesi et al. [21], who presented an adaptive heating curve for low temperature district heating systems. Lauenburg and Wollerstrand [10] developed a control algorithm to optimize supply temperatures of heating systems with oversized radiators. Huchtemann and Müller [22] presented an adaptive control algorithm which sets the supply temperature in discrete time steps depending on the position of the thermostatic valve. Tunzi et al. [23] dynamically optimized the mean logarithmic temperature difference of radiators to match the current heat demand and thus reduce return temperatures.

The previous research underlines the importance of low space heating temperatures for an energy-efficient operation of heat pumps. Several studies investigate the heat pump performance for specific systems [12–16], but comprehensive research is missing on the relationship between the design of the heat emission system with its nominal heating temperatures and heat pumps with their seasonal performance. We address this gap by the first research statement:

1) *What is the quantitative effect of (nominal supply and return) temperatures of the space heating circuit on the seasonal performance of heat pump systems?*

We investigate this research question by combining experimental data and simulation results of heat pump systems in existing buildings with radiators. Section 2 discusses dynamic temperatures in radiator heating systems and their effect on the performance of heat pump systems by analyzing field data of 49 retrofit heat pump systems in existing buildings. Section 3 systematically studies the correlation of heating temperatures and seasonal performance by means of detailed transient simulations of air source and ground source heat pump systems.

Depending on the installed radiators it might be necessary to make adoptions to the heating system for heat pumps to be viably applied. Several approaches have been discussed in the context of district heating networks to reduce return temperatures [9–11]. These approaches might also applicable but have not yet been adopted for heat pump systems. We therefore investigate the second research question:

2) *Which technical measures can be viably applied to reduce radiator temperatures in retrofit heat pump systems?*

We address this topic by applying and comparing two methods at the example of an existing multi-family building in Germany, and thus discuss their suitability for improving the performance of heat pump systems. Section 4 presents an analytical method, which determines required heating temperatures in renovated buildings, based on the reduced nominal heating load $\dot{Q}_{nom}$ and the heating temperatures in the unrenovated state. A second method in section 5 identifies critical radiators, which limit a further reduction of heating temperatures, by calculating the required heating load per room.

This approach of linking heat pump performance with methods to reduce heating temperatures allows to evaluate energy savings against refurbishment measures and thus design energy- and cost-efficient heat pump solutions for any existing building.

2. Analysis of temperatures and performance in heat pump systems

2.1. Heat pump characteristics

The coefficient of performance (*COP*) describes the instantaneous efficiency of heat pumps and is defined as the ratio of thermal power output $\dot{Q}_{HP}$ and electricity input P_{HP}:

$$COP = \dot{Q}_{HP}/P_{HP} \tag{1}$$

The heat pump output $\dot{Q}_{HP}$ can be also expressed as the sum of electricity input P_{HP} and input of ambient heat sources $\dot{Q}_{SRC}$:

$$\dot{Q}_{HP} = P_{HP} + \dot{Q}_{SRC} \tag{2}$$

The operating conditions influence the heat pump efficiency due to the nature of the underlying thermodynamic cycle. High temperatures of the heat source, i.e. the outdoor air temperature T_{air} in air source heat pumps, and the brine temperature T_{brine} in ground source heat pumps, and low supply temperatures $T_{sup,HP}$ are beneficial and yield a higher power output $\dot{Q}_{HP}$ and higher *COP*. By contrast, low source temperatures and high supply temperatures pose a challenge to heat pumps due to a drop of the Carnot efficiency.

Fig. 1 shows the performance maps of *COP* and thermal power of an air source heat pump (left) and a ground source heat pump

(right) as function of the source and supply temperature. Both heat pumps use the refrigerant R-410A as a working fluid.
The performance maps are derived from characterizing the heat pump performance at several stationary operation points with varying source and supply temperature according to DIN EN 14551:2013 [24]. The presented heat pump models are selected as market-average heat pump models with a rated efficiency of COP_{A2W35} = 3.8 of the air source heat pump and a COP_{B0W35} = 4.9 of the ground source heat pump. Hereby, the indices A2W35 and B0W35 stand for the nominal operating conditions with heat source temperatures of T_{air} = 2 °C, and T_{brine} = 0 °C, respectively, and a nominal supply temperature of $T_{sup,HP}$ = 35 °C.
The thermal power map in Fig. 1 depicts the heat pump output $\dot{Q}_{HP}$ at varying source and sink temperatures, relative to the power $\dot{Q}_{HP,nom}$ at nominal conditions. At elevated supply temperatures and low source temperatures, a reduction of the heat pump power $\dot{Q}_{HP}$ is observed, which is mainly due to a lower contribution of the ambient heat source $\dot{Q}_{SRC}$.
Furthermore, the graph shows the operating limits with regards to minimum and maximum temperatures of source and supply medium. The indicated operating limits are presented in the manufacturer's data sheet and are a limiting factor particularly during cold heating periods with low source temperatures and high supply temperatures.
Finally, the frequency distribution of operating conditions and the dynamics of the heat pump systems determine the annual energy performance.

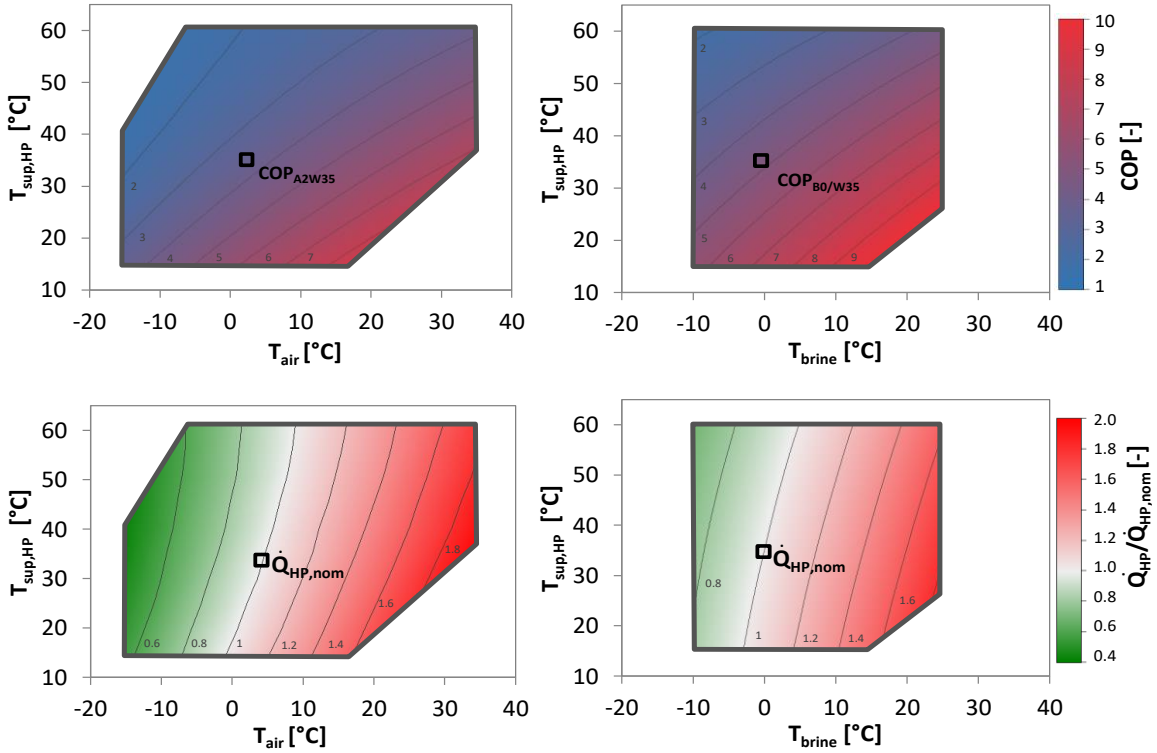

Fig. 1: Heat pump performance maps of *COP* (top) and relative heat pump power $\dot{Q}_{HP}/\dot{Q}_{HP,nom}$ (bottom) including operation limits as function of supply and source temperature (left: air source heat pump, right: ground source heat pump).

2.2. Radiator heat emission systems

Central hydronic heating systems are the predominant heating system in Europe. These systems transport heat via a heat transfer medium (hot water or steam) in closed circuits and transfer heat to the room via heating surfaces through a combination of convection and radiation [25].
Radiant floor heating systems have large heat transfer areas, thus achieve lowest heating temperatures and are therefore favorable for the application in heat pump systems. Radiator systems feature smaller heat transfer areas and therefore require higher supply temperatures to achieve the same heat output.
The first and second radiator equations describe the thermal output $\dot{Q}$ at varying operating conditions and can be used to convert the radiator heating power from any state 1 to state 2 [26,27]:

$$\frac{\dot{Q}_1}{\dot{Q}_2} = \frac{\dot{m}_1(T_{sup,1} - T_{ret,1})}{\dot{m}_2(T_{sup,2} - T_{ret,2})} \tag{3}$$

with the mass flow rate $\dot{m}$ per radiator, and the supply and return temperatures T_{sup} and T_{ret}.

$$\frac{\dot{Q}_1}{\dot{Q}_2} = \frac{A_1}{A_2} \cdot \left[\frac{\frac{T_{sup,1} - T_{ret,1}}{\ln\left(\frac{T_{sup,1} - T_{room,1}}{T_{ret,1} - T_{room,1}}\right)}}{\frac{T_{sup,2} - T_{ret,2}}{\ln\left(\frac{T_{sup,2} - T_{room,2}}{T_{ret,2} - T_{room,2}}\right)}} \right]^n \tag{4}$$

with the heat transfer area A, the air temperature of the room T_{room} and the radiator exponent n.

Therein, the indices 1 and 2 refer to two states, between which the conversion is be applied, e.g. to convert the heat output from state 1 at nominal radiator conditions to state 2 with reduced heating temperatures.
Note that Eq. (4) employs the logarithmic mean temperature difference. According to Albers [27], it is mandatory to use the logarithmic mean temperature difference instead of the algorithmic mean temperature difference, in case of large temperature gradients $(T_{ret} - T_{room})/(T_{sup} - T_{room}) < 0.7$. As the rated radiator power according to EN 442 is expressed at nominal conditions of T_{sup} = 75 °C, T_{ret} = 65 °C, and T_{room} = 20 °C, we use the more accurate, yet also more complex logarithmic mean temperature difference for all conversions.
Depending on the known and unknown parameters, an explicit solution is possible, or an implicit solution has to be derived.

2.3. Heating curve

Current heating systems actively control supply or return temperatures to meet the required heat demand while maintaining low temperatures to reduce heat losses and optimize the heat generator performance. Heating curves are a widely used approach that control heating temperatures as function of the outdoor temperature [27]. For an ideal heating system with a constant room temperature T_{room} the explicit heating curve is derived from the implicit radiator equations Eq. (2) and (3) and can be expressed as a function of the part load ratio $\dot{Q}_{rel}$ [28]:

$$T_{sup} = T_{room} + \left(\frac{T_{sup,nom} + T_{ret,nom}}{2} - T_{room}\right) \dot{Q}_{rel}^{\frac{1}{n}} + \frac{T_{sup,nom} - T_{ret,nom}}{2} \dot{Q}_{rel} \tag{5}$$

$$T_{ret} = T_{sup} - \dot{Q}_{rel}(T_{sup,nom} - T_{ret,nom}) \tag{6}$$

Hereby, the part load ratio $\dot{Q}_{rel}$ describes the relative heat load $\dot{Q}$ compared to the nominal heat load $\dot{Q}_{nom}$, which is given by the difference of outdoor air temperature T_{air} and heating limit temperature T_{lim}, i.e. the maximum outdoor air temperature which requires space heating:

$$\dot{Q}_{rel} = \frac{\dot{Q}}{\dot{Q}_{nom}} = \frac{T_{lim} - T_{air}}{T_{lim} - T_{air,nom}} \tag{7}$$

The nominal conditions refer to the design temperature $T_{air,nom}$ defining the lowest external air temperature for which the heating system must provide sufficient heat. Therefore, $T_{air,nom}$ depends on the climatic conditions and varies from location to location.
The nominal supply and return temperatures $T_{sup,nom}$ and $T_{ret,nom}$ describe the heating temperatures at design conditions, i.e. for $T_{air,nom}$. Regular operation typically occurs at higher air temperatures with a smaller part load ratio heat load, which allows lower heating temperatures T_{sup} and T_{ret} following Eq. (5) and (6).
"Real" heating curves, as implemented in heating controllers, consider additional aspects for a higher robustness: ambient temperatures are typically damped, e.g. by a moving average of past 24 h. Moreover, safety margins can be integrated to account for non-ideality factors. Increasing the nominal heating temperatures $T_{sup,nom}$ and $T_{ret,nom}$ yields a horizontal shift, while an increase of T_{lim} yields a vertical shift of the heating curve.
Fig. 2 plots the measured supply and return temperatures of an air source heat pump system in a small multi-family building with three apartments and radiator heat emission system located in the state of Hesse, Germany from the year 2018. The building was monitored scientifically within the project "WPsmart im Bestand" [29]. The lowest observed outdoor air temperature of T_{air} = -10.2 °C of that year lies above the nominal outdoor air temperature at the given location ($T_{air,nom}$ = -12.1 °C). The nominal heating temperatures ($T_{sup,nom}/T_{ret,nom}$ = 46.5 °C/41.8 °C) are therefore obtained by extrapolating the heating curve.
Fig. 2 also shows the corresponding hourly coefficient of performance *COP* and a histogram of normalized space heat supply as a function of the daily averaged outdoor air temperature. The histogram indicates the percentage of supplied space heat per 2 K interval of the outdoor air temperature with its distribution resembling a Gaussian distribution function with a median of T_{air} = 4.3 °C. The annual proportion of supplied space heat Q_{SH} at low outdoor air temperatures is remarkably small, although the space heating power $\dot{Q}_{SH}$ increases with colder outdoor air temperatures (compare Fig. 5). This effect is due to the fact that cold outdoor air temperatures occur rarely at the given location, so that 90 % of the space heat demand arise at outdoor air temperatures of -4 °C or above.
Note that the heat weighted mean supply and return temperatures amount to $T_{sup,mean}$ = 37.5 °C and $T_{ret,mean}$ = 32.2 °C, which is well below nominal conditions. Over the entire year, the heat pump achieves a seasonal performance factor for space heating of SPF_3 = 4.0, which can be interpreted as mean hourly *COP* values weighted with the relative frequency distribution of supplied space heat.
Most residential heat pump systems also deliver domestic hot water in addition to space heating. For the scope of this paper, however, we focus on space heating and neglect the influence of domestic water heating on heat pump operation and performance. Therefore, all specified indicators refer to space heating systems and exclude domestic water heating.

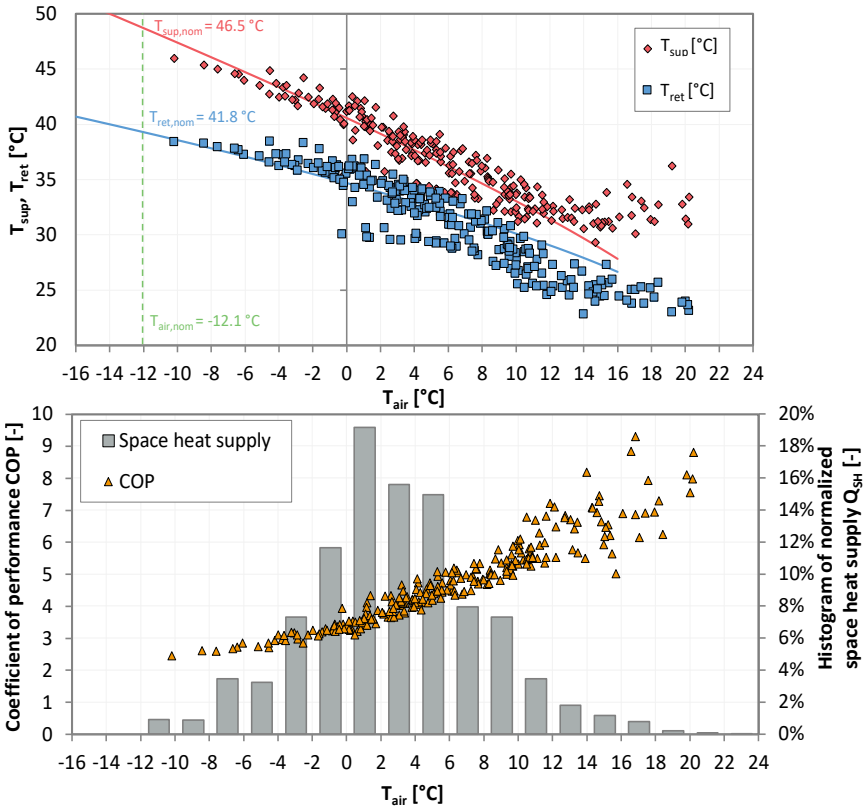

Fig. 2: Measured supply and return temperatures of a heat pump system with radiators (top) and the corresponding coefficients of performance and histogram of supplied space heat (bottom).

2.4. Seasonal performance factor SPF and mean heat pump temperature $T_{m,HP}$

The seasonal performance factor *SPF* characterizes the energetic performance of a heat pump system over a longer period, typically one heating period, and is defined as the ratio of the provided thermal energy to the consumed electrical energy. The *SPF* can be evaluated within different system boundaries. Throughout this paper, we use SPF_3 as key performance indicator of the heat pump system, which is defined analogously to SPF_{H3} in Zottl et al. [30] and includes the heat pump E_{HP}, backup unit E_{BU}, and pumps and ventilators on the source side E_{SRC} as electrical consumers (compare Fig. 6):

$$SPF_3 = \frac{Q_{HP} + Q_{BU}}{E_{HP} + E_{BU} + E_{SRC}} \tag{8}$$

The heat pump temperature in the condenser T_{HP} strongly affects the *COP* and the heat output $\dot{Q}_{HP}$ and is consequently a central operating condition affecting the electricity consumption. For a comprehensive understanding of the effective temperature level of the heat pump system, we define the mean heat pump temperature $T_{m,HP}$ as energy weighted annual average temperature:

$$T_{m,HP} = \frac{\int \frac{T_{sup,HP} + T_{ret,HP}}{2} \cdot \dot{Q}_{HP} dt}{\int \dot{Q}_{HP}\, dt} \tag{9}$$

$T_{m,HP}$ describes the mean temperature level of heat pump operation and thus characterizes the effective heat sink temperature averaged over a heating period. Fraga et al. [17] defined a similar indicator for the mean source temperature to correlate the *SPF* with various types of heat sources and their corresponding temperature level. In the context of solar thermal collectors, the characteristic temperature is used to assess PVT systems with regards to their mean operating temperature [30].

Analyzing the monitoring data from field measurement of 34 air source and 15 ground source heat pump systems shows a characteristic correlation between SPF_3 and $T_{m,HP}$. Fig. 3 plots the evaluated SPF_3 for space heating of the 49 heat pump systems over the mean heat pump temperature $T_{m,HP}$ for the heating period from July 2018 to June 2019. All buildings are located in Germany and employ a retrofit heat pump system, but differ regarding building size (mostly single-family houses, but also small multi-family buildings with up to four apartments), age, renovation standard, installed heat pump models, rated heat pump power, heat source temperature, and system control, just to name a few. Moreover, each of the 49 buildings feature its unique heating system ranging from radiant floor heating to radiator systems with the corresponding variation of nominal supply and return temperatures [29]. Due to the high variability of assessed systems, $T_{m,HP}$ ranges between 27.0 °C and 53.3 °C and SPF_3 between 1.5 and 5.4.

Despite the differences between the 49 systems, we can identify an approximately linear correlation between SPF_3 and $T_{m,HP}$ by means of linear regression. The R^2 statistic amounts to $R^2 = 0.71$ for the air source heat pump and to $R^2 = 0.60$ for the ground source heat pump. Given the large variations of the observed values of SPF_3, the R^2 statistics indicate that the linear regression is a good approximation for the analyzed data. The slope of the curves, i.e. the linear dependence of the seasonal performance

from the mean heat pump temperature, is of particular interest. For every Kelvin of lower $T_{m,HP}$, SPF_3 increases by 0.132 for the air source heat pump systems and by 0.103 points for the ground source heat pump systems. The indicated correlations in Fig. 3 allow an approximate calculation of SPF_3 based on the mean heat pump temperature. Therein, a reference temperature of 35 °C is chosen analogously to the definition of the supply temperature $T_{sup,HP}$, for which manufacturers state the rated parameters COP_{nom} and $\dot{Q}_{HP,nom}$.

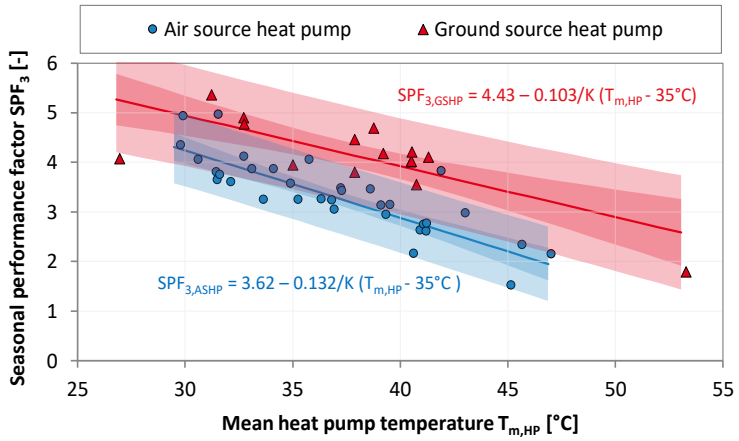

Fig. 3: Seasonal performance factor SPF_3 for space heating of 34 air source and 15 ground source heat pump systems from field measurements, with the underlying linear correlation and corresponding confidence (inner) and prediction (outer) intervals.

3. Simulation of heat pump systems with varying heating temperatures

In the following section, we study the effect of varying heating temperatures on the performance of heat pump systems using a detailed thermo-hydraulic simulation model of a heat pump system in a residential multi-family building.

3.1. Building physics and heat demand

The investigated multi-family building is located in Karlsruhe-Durlach in the south-west of Germany. The building was originally built in 1963 and renovated in 1995. We selected this building for this study due to its typical building geometry of a large multi-family building in the German building stock and for its characteristic building physics. The building forms part of a cluster of five similar buildings where an integrated energy system is developed and demonstrated within the research project "Smart district Durlach" [31].

The building features a heated floor area of 2112 m² on five floors with a total of 30 apartments (Fig. 4). In 1995, the building was renovated by exchanging the windows with insulating glazing (U_{win} = 1.7 W/m²K), and adding styrofoam layers of thermal insulation (d = 60 mm, λ = 0.035 W/mK) to the façade, cellar and ceiling, thus reducing the overall U-value of the opaque envelope from $U_{envelope}$ = 1.71 W/m²K to 0.36 W/m²K. Currently, a gas condensing boiler supplies the space heating and hot water demand. Tab. 1 summarizes the geometry and building physics of the studied building.

Fig. 4: Geometry and photo of the studied building in Karlsruhe-Durlach.

Tab. 1: Geometry and building physics of the studied building.

	Symbol	Unit	Parameter
Reference floor area	A_{floor}	m²	2112
Net ground floor area	A_{net}	m²	2182
Heated volume	V_{heated}	m³	5683
Façade area (excl. windows)	$A_{envelope}$	m²	1503
Cellar area	A_{cellar}	m²	563

Upper ceiling area	$A_{ceiling}$	m²	563
U-value envelope	$U_{envelope}$	W/m²K	0.36
Area of windows and doors	$A_{windows}$	m²	232
U-value windows	$U_{windows}$	W/m²K	1.7
G-value of windows	$g_{windows}$	-	0.75
Air changes per hour	ACH	1/h	0.70
Internal heat gains	$\dot{q}_{internal}$	W/m²	1.5

We model the building and its space heating demand by a thermal building model that is based on EN ISO 13790:2008 [32]. It considers heat transfer by transmission and ventilation, as well as solar and internal gains. A dynamic 5R2C network regards all apartments as a single thermal zone, which is justified given their similar room temperatures and utilization profiles.
Weather data from the Meteonorm database for a typical meteorological year for Karlsruhe is used. The simulated heat demand is shown in Fig. 5 with a specific heat demand of Q_{SH} = 64.7 kWh/m²a, a nominal heating power of $\dot{Q}_{SH,nom}$ = 77.8 kW, and a heating limit of T_{lim} = 16.2 °C. The simulated data corresponds well with detailed measurements of the real building in the heating period in the year 2019 where a nominal heat power of $\dot{Q}_{SH,nom}$ = 76.2 kW at the nominal outdoor temperature $T_{air,nom}$ = -12 °C and a heating limit of T_{lim} = 16.4 °C are extrapolated from measurement data. Furthermore, a temperature-corrected specific heat demand of Q_{SH} = 58 kWh/m²a is derived from consumption data over five years of operation [33].

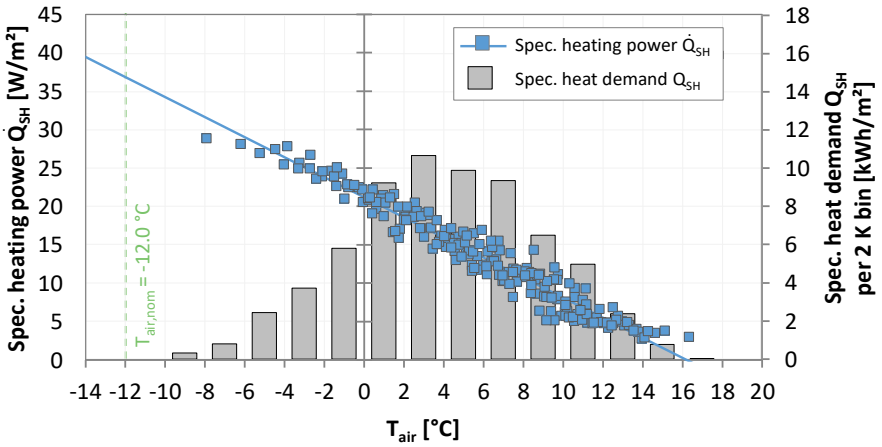

Fig. 5: Daily heating power $\dot{Q}_{SH}$ and histogram of specific heat demand Q_{SH} as function of the outdoor air temperature.

3.2. Simulation framework

We model a complete air source and ground source heat pump system including backup unit, buffer storage, hydraulics, control, and the radiator heat emission system. The heat pump system is implemented in Dymola/Modelica allowing a detailed thermohydraulic simulation with realistic control methods. Fig. 6 depicts the corresponding hydraulic layout with the respective definitions of temperatures as well as thermal and electrical energy flows $\dot{Q}$ and P.

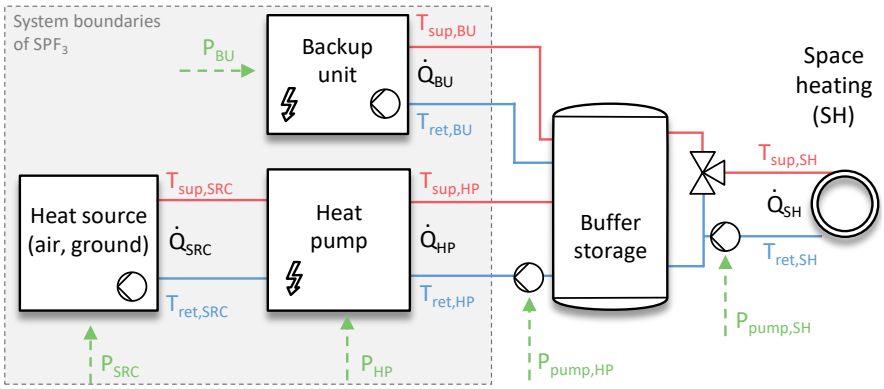

Fig. 6: Simplified hydraulic layout of the modelled heat pump system.

A nominal thermal heat pump power of $\dot{Q}_{HP,nom}$ = 54.2 kW_{th} is assumed for the air and ground source heat pump. For the transient simulation, the performance maps of COP and $\dot{Q}_{HP}$ as function of source and supply temperatures according to Fig. 1 with corresponding temperature limits are used. Thus, the instantaneous heat pump performance is modelled accurately during every time step. Dymola uses a solver with variable time step intervals.
The heat pumps are sized to cover the total heat demand at outdoor air temperatures above T_{air} = -4 °C, which corresponds to a share of 95 % of the annual heat demand. A backup unit runs in parallel as secondary heat generator and covers the residual heat load in periods, when the heat pump power $\dot{Q}_{HP}$ is insufficient to provide the heat demand $\dot{Q}_{SH}$ or when the heat pump is unable

to deliver the required supply temperatures $T_{sup,SH}$. The backup unit is modelled as ideal electrical heater with a conversion efficiency of η = 100 %. Most systems in multi-family buildings would employ a gas heating backup system. For reasons of comparability, however, we study this monoenergetic system and thus simplify the following analysis of seasonal performance factors.

The operation of the fixed speed heat pump is controlled by a PI controller with hysteresis to suppress cycling. The controller starts the heat pump when the storage temperature at a relative height of 0.8 falls below the requested supply temperature $T_{sup,SH}$, according to the heating curve, within a hysteresis threshold of 4 K. The backup unit only provides the residual heat demand when the heat pump is unable to deliver sufficient temperatures or power. For that purpose, the modulating backup heater is controlled by a secondary, subordinate PI controller.

For the parametrization of the heating curve, a temperature limit of T_{lim} = 20° C is considered in contrast to the heating limit of T_{lim} = 16.2 °C of the modelled building. This offset corresponds to a more realistic approximation of real heating curves as implemented on heat pump system controllers in field applications.

Component models are used from the openly accessible libraries Buildings [28], AixLib [34], and IBPSA [35], except for the self-developed ground heat exchanger model, which uses a vertically and radially discretized ground temperature profile and calculates the dynamic heat exchange between each fluid and ground node assuming a constant heat transfer coefficient. Tab. 2 summarizes the relevant component models and their central parameters. A sensitivity analysis for pivotal parameters was conducted showing that the simulation results are robust. For example, a variation of the number of nodes n_{nodes} in the buffer storage within a range of 50 % - 300 % leads to a marginal variation of the SPF_3 of only ± 0.5 %.

Tab. 2: Components and models used for the simulation of the heat pump system in Dymola/Modelica.

Component	Modelica model	Parameters
Heat pump	HeatPump (AixLib)	Air source heat pump (ASHP): $\dot{Q}_{HP,nom}$ = 54.2 kW_{th} (A2/W35) COP_{A2W35} = 3.8 $T_{cond,max}$ = 60.0 °C Ground source heat pump (GSHP): $\dot{Q}_{HP,nom}$ = 54.2 kW_{th} (B0/W35), COP_{B0W35} = 4.9 $T_{cond,max}$ = 60.0 °C
Buffer storage	BufferStorage (AixLib)	$V_{storage}$ = 1 m³ *nNodes* = 10
Controller (HP and backup unit)	PIDHysteresisTimer (Buildings)	PI Controller with k_P=0.125, T_I = 10.6 s
Heating curve	HotWaterTemperatureReset (Buildings)	$T_{room,nom}$ = 20 °C T_{lim} = 20 °C $T_{air,nom}$ = -12 °C
Radiators	RadiatorEN442_2 (IBPSA)	Radiator exponent n = 1.3 Radiator areas sized to meet design heat load
Ground heat exchanger	GroundHX (own model)	Double U-pipe ground heat exchanger 12 probes with each 90 m length
Weather	TMY3Reader (Buildings)	Location: Karlsruhe, Germany. Source: Meteonorm

3.3. Simulation results

To analyze the isolated effect of heating temperatures, we simulate the annual performance of the air source and ground source heat pump systems at varying nominal supply and return temperatures $T_{sup,nom}/T_{ret,nom}$ of the space heating circuit. In this parametric study, only the settings specifying the space heating system are varied, i.e. the size and capacity of the radiators. All remaining parameters, i.e. building heat demand, heat pump power, component sizes and controller settings, are kept constant. Fig. 7 plots the resulting seasonal performance factor SPF_3 over the mean heat pump temperature $T_{m,HP}$ for varying heating temperatures.

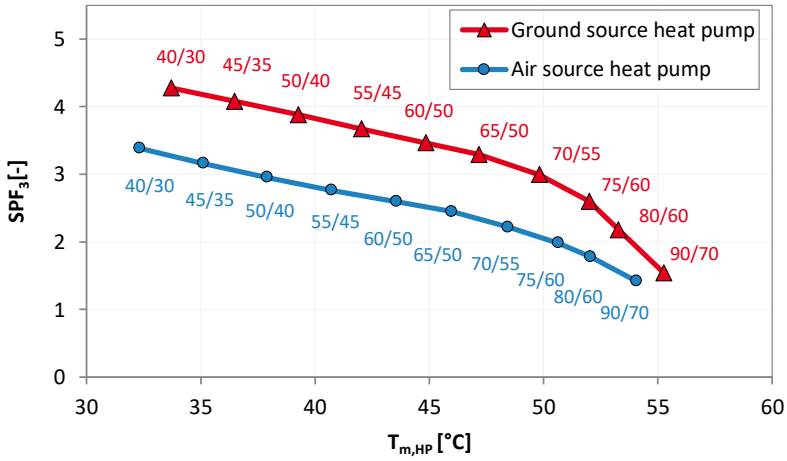

Fig. 7: Seasonal performance factor SPF_3 at varying nominal supply and return temperatures $T_{sup,nom}/T_{ret,nom}$ of the space heating circuit.

The indicated nominal supply and return temperatures $T_{sup,nom}/T_{ret,nom}$ characterize the heating curve settings and thus the underlying configuration of the radiator heating system. Heating systems with large radiator areas can be operated at low system temperatures, whereas systems with smaller radiators areas must compensate their lower capacity by increasing the system temperatures.

The seasonal performance factor SPF_3 increases with lower system temperatures due to a higher COP and due to a smaller share of the backup heating system. Comparing the heat pump technologies in absolute terms, shows that the GSHP achieves a SPF_3 of 0.9 points above the ASHP. Both curves are in good agreement with the experimental results from the field measurements in Fig. 3. On average, SPF_3 increases by 0.1 points for each Kelvin of lower mean heat pump temperatures until the curve bends distinctly above $T_{m,HP}$ = 50 °C.

Fig. 7 also shows the relationship of nominal heating temperatures and the energy-weighted mean heat pump temperature. $T_{m,HP}$ results from the dynamic operation of the heat pump in interaction with the storage and the control strategy, particularly the heating curve. Fig. 8 plots $T_{sup,SH}$ as function of T_{air} according to the corresponding heating curve settings at nominal conditions (compare equations (5) - (7)). At the given location, the histogram of Q_{SH} indicates that 90 % of the space heat demand occurs in the air temperature range between -4 °C and 12 °C, with a mean outdoor air temperature of delivered heat of $T_{m,air}$ = 3.4 °C. Accordingly, this is the temperature range most relevant concerning heat pump performance.

Although the simulated seasonal performance factors in Fig. 7 are only valid for the studied building, the central findings can be transferred to other buildings. A sensitivity study for a single-family house with a smaller heat demand yields a similar curve with only marginal differences of SPF_3. The building location, its climate, and the corresponding nominal outdoor temperatures, however, influence the heating curve and the frequency distribution of Q_{SH}. Therefore, referring SPF_3 to the mean heat pump temperature $T_{m,HP}$ is a practical method to systematically assess the influence of condenser temperatures, and consequently heating temperatures, on the heat pump performance.

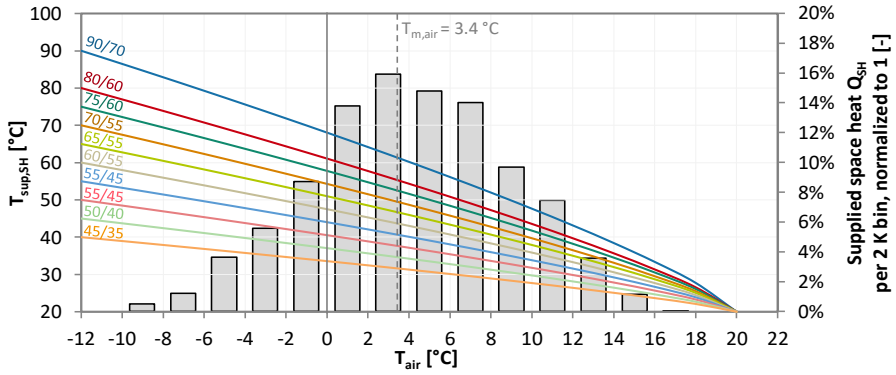

Fig. 8: Supply temperature of space heating $T_{sup,SH}$ for different heating curves in relation to the histogram of supplied space heat Q_{SH}.

Fig. 9 analyzes the energy balance of a full heating period in more detail, indicating the different contributions of heat pump electricity E_{HP}, ventilator and pump energy on the source side E_{SRC}, energy for the backup unit E_{BU}, and ambient heat from the environmental source Q_{SRC}. The specific values are given relative to the heated floor area A_{floor}.

With increasing heating temperatures, an increase of the relative share of electricity is observed. The underlying reason is found in the COP performance maps in Fig. 1. With higher supply temperatures, less low-temperature heat from the ambient heat sources Q_{SRC} is utilized. Especially in combination with low source temperatures $T_{sup,SRC,}$ this causes the heat pump to underperform, resulting in a larger share of $E_{HP.}$ Moreover, the heat pump is unable to cover the space heating demand alone, which is why the relative share of E_{BU} increases. Furthermore, the required supply temperatures $T_{sup,SH}$ frequently exceed the maximum condenser temperature $T_{cond,max}$, resulting in an increasing utilization of the backup unit. As a combined result of these effects, the curve of SPF_3 drops distinctly above nominal heating temperatures of 70°C/55°C.

At elevated heating temperatures, it would be therefore favorable to employ alternative heat pump technologies which allow

higher condenser temperatures. A bivalent system with backup gas heater and a smaller share of heat supplied by the heat pump might also constitute a feasible alternative.

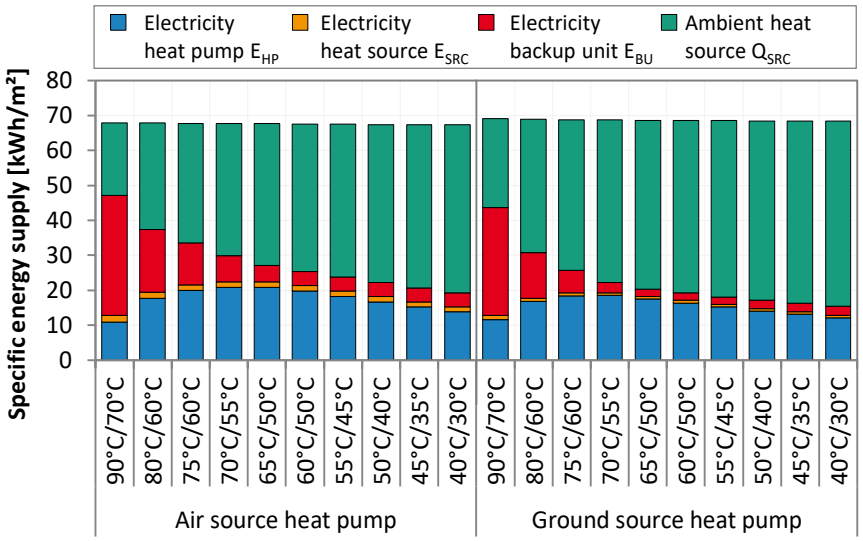

Fig. 9: Annual contributions of specific energy supply for air source and ground source heat pump systems at varying nominal supply and return temperatures $T_{sup,nom}/T_{ret,nom}$.

4. Analytical method to determine required heating temperatures based on renovation state

4.1. Method

Energy renovation in buildings, e.g. improving the thermal insulation of the façade or replacing windows, aims at reducing the building's transmission losses and thus the demand for space heating Q_{SH}. Due to the corresponding lower heat load $\dot{Q}_{nom}$, the required heating temperatures can be lowered without changing the heat emission system. The following analytical approach derives the required nominal supply and return temperatures from the original heating temperatures in the unrenovated state. In doing so, this method allows to estimate the effect of energy renovation on nominal heating system temperatures and consequently the energetic performance of the heat pump system.

Although the radiator equations (3) and (4) describe single radiators, they can be applied to an entire building and its heat emission system. This simplification reduces the building with its multiple rooms and radiators to a single node. Heinz and Rieberer [18] apply a similar approach, treating the building as a single thermal zone with only one equivalent radiator.

Assuming identical radiators (i.e. $A_1 = A_2$), constant mass flow rates ($\dot{m}_1 = \dot{m}_2$) and equal room temperatures ($T_{room,1} = T_{room,2}$), the radiator performance can be converted from the unrenovated state 1 with the nominal heat load $\dot{Q}_{nom,1}$ to the renovated state 2 with the reduced heat load $\dot{Q}_{nom,2}$. With these assumptions, the following explicit correlations are derived from the implicit radiator equations applying basic algebraic rules and solving the equation system to $T_{sup,2}$:

$$T_{sup,2} = T_{room,2} + \Delta T_2 \frac{exp\left(\frac{\Delta T_2}{\Delta T_{log,2}}\right)}{exp\left(\frac{\Delta T_2}{\Delta T_{log,2}}\right) - 1} \tag{10}$$

with the temperature difference ΔT_2:

$$\Delta T_2 = T_{sup,2} - T_{ret,2} = (T_{sup,1} - T_{ret,1}) \frac{\dot{Q}_{nom,2}}{\dot{Q}_{nom,1}} \tag{11}$$

and the logarithmic temperature difference $\Delta T_{log,2}$:

$$\Delta T_{log,2} = \frac{T_{sup,2} - T_{ret,2}}{\ln\left(\frac{T_{sup,2} - T_{room,2}}{T_{ret,2} - T_{room,2}}\right)} = \frac{T_{sup,1} - T_{ret,1}}{\ln\left(\frac{T_{sup,1} - T_{room,1}}{T_{ret,1} - T_{room,1}}\right)} \sqrt[n]{\frac{\dot{Q}_{nom,2}}{\dot{Q}_{nom,1}}} \tag{12}$$

The return temperature of the renovated heating system is then given by $T_{ret,2} = T_{sup,2} - \Delta T_2$.

Fig. 9 depicts the correlations of equations (10) - (12) for four ratios of design heat load after and prior to renovation $\dot{Q}_{nom,2}/\dot{Q}_{nom,1}$, illustrating the potential to reduce heating temperatures depending on the renovation level.

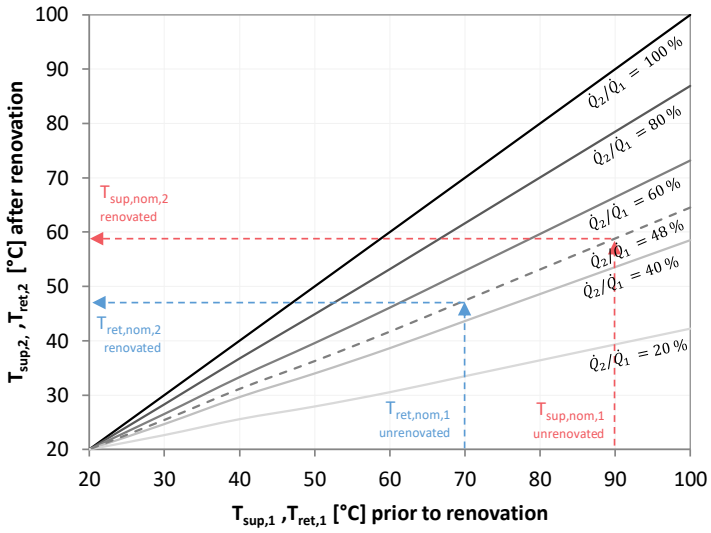

Fig. 10: Reduction of supply and return temperatures for four different renovation states $\dot{Q}_2/\dot{Q}_1$ and for the example of the Karlsruhe-Durlach building with $\dot{Q}_{nom,2}/\dot{Q}_{nom,1} = 48\%$, T_{room} = 20 °C, n = 1.3.

Due to the underlying simplifications, this analytical method can only serve as a first estimation of a temperature range for nominal heating temperatures. However, as only the ratio of design heat loads $\dot{Q}_{nom,2}/\dot{Q}_{nom,1}$ and the nominal heating temperatures of the unrenovated building are required inputs, the simplicity also has its advantages with regards to a quick and general applicability. A more comprehensive approach, which follows a detailed heat load analysis per room, is presented in section 5.

4.2. Case study for the reference multi-family building

This method is exemplarily applied for the reference building in Karlsruhe-Durlach. Prior to its renovation in 1995, the building had a design heat load of $\dot{Q}_{nom,1}$ = 138 kW and presumably $T_{sup,nom,1}$ = 90 °C and $T_{ret,nom,1}$ = 70 °C. Due to the described energy renovation measures, the nominal heat load was reduced to $\dot{Q}_{nom,2}$ = 66 kW, or to 48% of the initial heat load.
The example case with $\dot{Q}_2/\dot{Q}_1 = 48$ % is shown by the dashed lines in Fig. 9. With the assumptions of T_{room} = 20 °C and n = 1.3, the nominal heating temperatures can be reduced to $T_{sup,nom,2}$ = 58.8 °C and $T_{ret,nom,2}$ = 49.2 °C. The currently installed heating system with gas boiler operates on a heating curve with nominal heating temperatures of 80°C/65°C. This suggests that there is an unexploited potential to reduce heating temperatures by lower heating curve settings without risking an undersupply of heat.

5. Method to identify critical radiators for selective exchange

5.1. Method

The following method assesses the required heating system temperatures on room level, as opposed to the building level in the previous section. For that purpose, we compare the design heat load per room with the heating power of the installed radiators at varying system temperatures.
Instead of exchanging the entire heat emission system, it may suffice to selectively exchange those bottleneck radiators that determine the maximum system temperatures. Østergaard and Svendsen [11] developed a similar method to identify critical radiators by calculating a required logarithmic mean temperature difference ΔT_{log} per radiator, which should ideally match the average ΔT_{log} required in the building.
With the following five steps, critical radiators, which limit a further reduction of heating temperatures, can be identified:

1) Calculate the design heat load per room $\dot{Q}_{room}$ based on building geometry, building physics, occupant behavior and nominal conditions, e.g. according to EN 12831-1:2017 [36].
2) Ascertain the installed radiators and their heating power at nominal conditions $\dot{Q}_{rad,nom}$. The nominal heating power of the radiator inventory can be obtained from manufacturer data sheets based on radiator size, type and method of installation.
3) Convert the radiator heating power from nominal conditions to reduced heating temperatures $\dot{Q}_{rad,T_{sup}/T_{ret}}$. The radiator heating power is typically stated at nominal conditions $T_{sup,nom}$ = 75 °C, $T_{ret,nom}$ = 65 °C, T_{room} = 20 °C. This nominal power can be converted to any set of operating conditions by application of the second radiator equation in Eq. (4). Hereby, the individual hydraulic situation of each radiator has to be considered. In parallel strings, a hydronic balancing valve is required to ensure equal flow and temperatures over all strings and radiators. In serial strings, the supply and return temperatures per radiator has to be considered taking into account the temperature drop over each radiator.
4) Compare the radiator power at the reduced heating temperature level $\dot{Q}_{rad,T_{sup}/T_{ret}}$ with the room's heat load $\dot{Q}_{room}$ and assess violation of thermal comfort. The radiator power at reduced heating temperatures must be equal or larger than the design heat load of the room to fulfil thermal comfort requirements, i.e. $\dot{Q}_{rad,T_{sup}/T_{ret}}/\dot{Q}_{room} > 1$.

5) Identify critical radiators. Radiators should be exchanged in those rooms, where the radiator power is insufficient to meet the room's design heat load. Instead of new radiators with larger heat transfer area, it is also possible to equip the critical radiators with convectors to enhance the convective heat transfer and thus increase their power.

Repeating step 3) to 5) for different values of $T_{sup,nom}/T_{ret,nom}$ identifies critical radiators and determines the number of undersized radiators for each set of heating temperatures. The interested reader may refer to Østergaard and Svendsen [11] for a more detailed explanation of the method, or to Jagnow et al. [37] for a detailed guideline of optimizing radiator systems in existing buildings.

5.2. Case study for the reference multi-family building

The potential to reduce heating temperatures by selectively exchanging single radiators strongly depends on the building physics. Previous studies [9,11] for buildings connected to district heating networks in Denmark and Sweden, however, indicate that return temperatures can be reduced significantly by a detailed analysis of the radiator systems. We now apply the method to identify critical radiators for two types of multi-family buildings within the Karlsruhe-Durlach district.

Building type 1 is the building described in section 3.1, which features 150 heated rooms on a heated floor area of A = 2112 m^2 with 21 different types of radiators. Building type 2 features 180 heated rooms on a heated floor area of A = 2540 m^2, with 8 different types of radiators. Both buildings were constructed and renovated in the same year and feature similar building physics. However, the nominal power of the installed radiators differs substantially between both buildings (116 W/m$^2_{floor}$ in building 1 compared to 89 W/m$^2_{floor}$ in building 2).

The design heat load per room is calculated according to EN 12831-1:2017 [36] on the basis of detailed room and building data. Nominal room temperatures of T_{room} = 20 °C are assumed for all rooms, except for living rooms with 22 °C, and bathrooms with 24 °C. Fig. 11 compares the design heat load per room with the heating power per radiator at different heating temperatures for building type 1. The critical radiators with insufficient power in the red area must be exchanged to reduce heating system temperatures of the entire building.

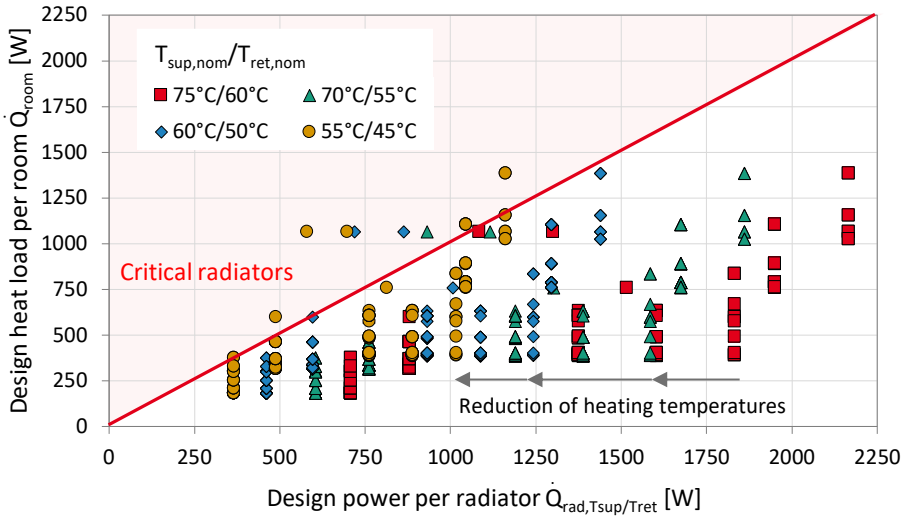

Fig. 11: Comparison of heat load per room $\dot{Q}_{room}$ and radiator power $\dot{Q}_{rad}$ at varying heating temperatures $T_{sup,nom}/T_{ret,nom}$ in building type 1. All radiators above the red line are undersized and must be exchanged for a reduction of heating temperatures.

According to the analysis, all radiators are sized sufficiently to reduce the heating system temperature to 75°C/60°C and only one out of 150 radiators must be replaced to achieve 70°C/55°C. A further reduction to 55°C/45°C requires an exchange of 7 % of all existing radiators. These critical radiators are mostly found in bathrooms, corner rooms with two outdoor walls, and on the first and top floor.

Despite the similarities with building type 1, the analysis shown in Tab. 3 paints a different picture for building type 2. In this building type, 6 % of all radiators must be exchanged to achieve system temperatures of 70°C/55°C. To reduce temperatures to 55°C/45°C, this applies to more than 50 % of all radiators.

The different rate of critical radiators is due to the fact that the installed nominal radiator power capacity in building type 1 is 30 % larger than in building type 2 . These significant differences most likely originate from a different approach that was applied for the original sizing of the radiator heat emission system. Therefore, reduction of heating temperatures requires a detailed look at the building specifics and a consideration of the individual radiator types and rated heating power.

Tab. 3: Number of critical radiators for two types of building in the Karlsruhe-Durlach district and corresponding seasonal performance factors.

System temperatures $T_{sup,nom}/T_{ret,nom}$	Building type 1		Building type 2		Seasonal performance factor SPF_3	
	Critical radiators (total of 150)		Critical radiators (total of 180)		ASHP	GSHP
75°C/60°C	0	0 %	0	0 %	2.0	2.6
70°C/55°C	1	0.7 %	10	6%	2.3	3.0
65°C/50°C	2	1.3 %	18	10%	2.5	3.4
60°C/50°C	3	2 %	64	36%	2.7	3.5
55°C/45°C	11	7 %	94	52%	2.8	3.7
50°C/40°C	44	29 %	138	77%	3.0	4.0

5.3. Economic assessment of the selective radiator exchange

To economically assess the measure of exchanging radiators, we compare the levelized costs of heat *LCOH* based on the annuity of investment costs *ANI*, annual maintenance costs *AMC*, and annual energy costs *AEC* for all studied cases.

The investment costs for the radiator exchange are given by the number of radiators n_{rad} to be exchanged multiplied by the costs per radiator of $I_{0,rad}$ = 630 €, which comprise material costs of 352 € and installation costs of 278 €. The specific investment costs for the heat pump including installation amount to $I_{0,HP}$ = 739 €/kW$_{th}$. Specific investment costs for the heat source are estimated at $I_{0,SRC}$ = 286 €/kW$_{th}$ for the outdoor air unit and at $I_{0,SRC}$ = 1436 €/kW$_{th}$ for the geothermal probes. All net cost figures are obtained from manufacturer's and installer's quotes for the Karlsruhe-Durlach district.

The assessment of investment costs is carried out with the annuity method, which converts the initial investment costs I_0 to a corresponding annuity of the investment *ANI*:

$$ANI = \left[n_{rad} \cdot I_{0,rad} + \dot{Q}_{HP} \cdot I_{0,HP} + \dot{Q}_{SRC} \cdot I_{0,SRC}\right] \frac{(1+i)^n i}{(1+i)^n - 1} \quad (13)$$

with an assumed interest rate of i = 3 %, and a considered lifetime of n = 20 years. Annual maintenance costs *AMC* for the heat pump and heat source system are considered at an annual rate of 2.5 % of the initial investment costs.

The annual energy costs *AEC* cover the purchase of electricity for the operation of the heat pump, backup unit and auxiliaries:

$$AEC = c_{el}(E_{HP} + E_{BU} + E_{SRC}) \quad (14)$$

with an assumed electricity price varying in the range of c_{el} = 20 - 35 ct€/kWh$_{el}$.

The resulting levelized costs of heat *LCOH* are given by the sum of annual costs divided by the delivered space heat Q_{SH} [38]:

$$LCOH = \frac{ANI + AMC + AEC}{Q_{SH}} \quad (15)$$

For the scope of this assessment, investment costs for storages and backup units are not regarded and constant annual heat generation and operating costs are assumed. Note that the levelized costs of heat of bivalent systems with a backup gas boiler, or systems with additional domestic water heating may differ considerably.

Fig. 12 shows the breakdown of the levelized costs of heat for an air and ground source heat pump in building type 1 and 2. With lower heating temperatures, the investment costs increase as more radiators are exchanged, whereas the energy costs decrease due to a higher SPF_3. The annual energy costs for the ground source heat pump systems are substantially smaller due to their lower electricity consumption, but investment costs are higher.

In building type 1, both heat pump technologies reach the cost optimum at heating temperatures of 55°C/45°C. To achieve these nominal heating temperatures, 7 % of all installed radiators are renewed, which accounts for a share of only 2 % of annual costs. Hence, the savings of energy costs outweigh the investment for the radiators, and a relative reduction of heating costs of 10 % - 24 % is observed, depending on electricity prices. A further temperature reduction achieves additional energy cost savings, which, however, cannot offset the higher investment for the radiators.

Although building type 2 requires a larger share of radiators to be exchanged, cost savings are also achieved in this building. The cost optimum for most cases is achieved at nominal heating temperatures of 65°C/50°C, where 10 % of all radiators are exchanged. Despite the larger number of exchanged radiators, a relative reduction of heating costs in the range of 4 % - 14 % is observed in building type 2.

In conclusion, the selective radiator exchange is both a cost- and energy-efficient measure, which requires minimal changes to the building and its heat emission system. Especially air source heat pump systems achieve significant cost and energy savings from applying this method. We therefore recommend including this method in the planning and design process of heat pump systems and analyze the specific potential to reduce heating temperatures in the individual building.

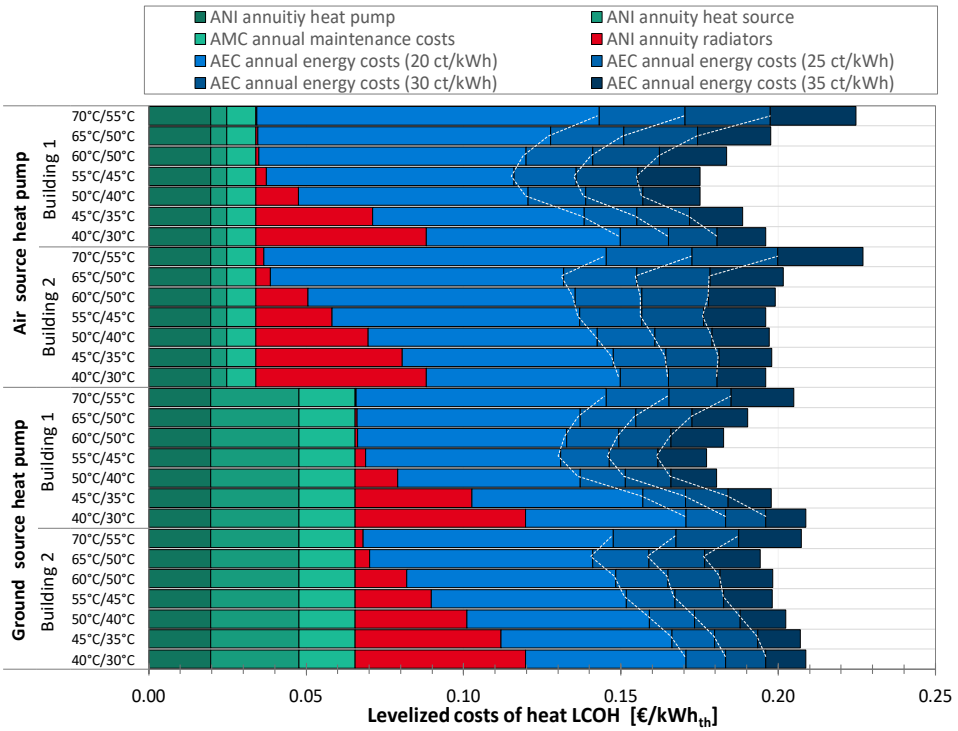

Fig. 12: Breakdown of levelized costs of heat LCOH into annual costs of investment *ANI* (heat pump, heat source, radiator exchange), annual maintenance costs *AMC* and annual energy costs *AEC* for varying electricity costs of c_{el} = 20 – 35 ct/kWh$_{el}$.

6. Discussion

6.1. Effect of heating temperatures on the seasonal performance of heat pumps via $T_{m,HP}$

The novel indicator $T_{m,HP}$ describes the mean temperature level of heat pump operation. As the instantaneous coefficient of performance *COP* is a function of the supply temperature $T_{sup,HP}$, we are interested in the mean heat pump temperature, which affects the seasonal performance over an entire heating period. $T_{m,HP}$ takes the frequency of temperatures into account by weighting the mean condenser temperature with the thermal power, and thus characterizes the average temperature level of delivered heat. Having said that, it can be interpreted as the mean operating temperature level of the heat pump condenser, which principally affects the seasonal performance. Thus, $T_{m,HP}$ can be considered as the central link between the building's heat emission system and the performance of the heat pump system.

Analyzing field data of the performance of 49 existing retrofit heat pump systems reveals a linear correlation between the mean heat pump temperature $T_{m,HP}$ and the seasonal performance factor SPF_3. According to the correlation, every Kelvin of reduced $T_{m,HP}$ increases the SPF_3 by 0.13 points (air source heat pump) and by 0.10 points (ground source heat pump). Given the high number and diversity of analyzed systems, these values can be considered representative for current heat pump systems.

By means of detailed dynamic system simulations, the isolated effect of varying nominal heating temperatures and their corresponding heating curve on seasonal performance is studied. Good agreement with experimental results is found and the simulation results lie within the prediction interval of the experimental correlation. At nominal heating temperatures above 65°C/50°C, the seasonal performance drops distinctly as the heat pumps frequently reach their operation limit (compare Appendix A).

Hence, the findings from field measurements and system simulations support the hypothesis that low space heating temperatures are essential for an energy-efficient operation of heat pump systems. Moreover, the presented method provides a systematic, quantitative basis for analyzing the effect of heating temperatures on system performance, based on $T_{m,HP}$.

6.2. Measures to reduce radiator temperatures

Two technical measures to reduce temperatures in the space heating circuit of radiator systems were presented:

1) Thermally insulating the building envelope leads to a reduction of the building's transmission losses. Due to the lower design heat load, temperatures can be reduced using the existing radiators. Analytical correlations, derived from the radiator equations, allow an estimate of heating temperatures in renovated buildings, based on the original heating temperatures and the level of renovation.
2) A more detailed method assesses the required heat demand and the installed radiator capacity per room. Radiators in existing buildings are often oversized and single radiators with insufficient heating power limit a further reduction of heating temperatures. The selective exchange of those critical radiators constitutes an effective measure to reduce nominal heating temperatures without exchanging the entire heat emission system.

Both methods are applied exemplarily for two existing multi-family buildings in Germany to illustrate their application and demonstrate their potential. Tab. 4 compares the results applied to both building types. By linking these results with the previous

simulations, the effect of each measure on the mean heat pump temperature $T_{m,HP}$ and the seasonal performance factor SPF_3 can be compared.

Thermal insulation reduces the nominal heat load to 48 % of the state prior to renovation. According to the method on building level in section 4, the nominal supply and return temperatures of the space heating circuit can be reduced to 60°C/50°C. However, a detailed heat load calculation on room level shows that the installed radiators only allow a reduction to 75°C/60°C. Some radiators have an insufficient capacity relative to their room's heat load and therefore limit a reduction of heating temperatures to the levels obtained by the method on building level. Assessing heating temperatures on building level therefore cannot substitute the detailed assessment on room level and should be only applied to preliminarily estimate average heating temperature levels.

A large potential to reduce temperatures can be exploited by analyzing heat load and radiator capacity on room level with the aim to identify and exchange critical radiators, which limit a further reduction of system temperatures. In building type 1, the selective exchange of only 7 % of all radiators is sufficient to reduce the nominal heating temperatures from 75°C/60°C to 55°C/45°C. This corresponds to an increase of SPF_3 from 2.0 to 2.8 (air source heat pump) and from 2.6 to 3.7 (ground source heat pump), or a reduction of the electricity consumption of 40 % - 42 %, respectively. Despite their similarities in age and building physics, the effect of the selective exchange is significantly lower in building type 2. Therein, exchanging 10 % of all radiators only yields temperature reduction to 65°C/50°C.

The suitability of the method is therefore specific to each individual building, depending on its renovation state and the heat transfer capacity of installed radiators. Radiators are often installed in standard sizes and varying safety margins are considered. Moreover, insulating the building envelope might lead to a disproportional reduction of the heat load in different rooms, with some rooms experiencing a larger relative reduction the heat load than others [37]. These factors ultimately affect the rate of undersized radiators that require an exchange to reduce heating temperatures to specific temperature levels.

Nonetheless, the economic assessment of the method illustrates its large potential as energy and cost-efficient measure to reduce heating temperatures. Thus, this study supports the findings by Østergaard and Svendsen [11] and Jangsten et al. [9], and transfers the methods from the context of district heating networks to heat pump systems. The results illustrate that it is worthwhile to apply this method in the design process of retrofitting heat pumps to existing buildings with radiator heating systems.

Tab. 4: Comparison of measures to reduce heating temperatures and their effect on the mean heat pump temperature $T_{m,HP}$ and seasonal performance factor in building type 1 and 2.

	Technical measures to reduce heating temperatures	$T_{sup,nom}$/ $T_{ret,nom}$	**Air source heat pump**			**Ground source heat pump**		
			$T_{m,HP}$	SPF_3	**Electricity savings**	$T_{m,HP}$	SPF_3	**Electricity savings**
Building 1	1) Original	90°C/70°C	54.1°C	1.4	-	55.3°C	1.6	-
	2) Reduced heat load (48 %)	75°C/60°C	50.6°C	2.0	40%	52.0°C	2.6	69%
	3) Exchange of radiators (7 %)	55°C/45°C	40.7°C	2.8	40%	42.0°C	3.7	42%
Building 2	1) Original	90°C/70°C	54.1°C	1.4	-	55.3°C	1.6	-
	2) Reduced heat load (48 %)	75°C/60°C	50.6°C	2.0	40%	52.0°C	2.6	69%
	3) Exchange of radiators (10 %)	65°C/50°C	46.0°C	2.5	24%	47.2°C	3.4	27%

6.3. Outlook: implementation of heat pump systems in the case study district

Based on the previous considerations, the following integrated energy system is implemented in the case study district in Karlsruhe-Durlach. The district consists of five residential multi-family buildings, of which two belong to building type 1 and three to building type 2.

Decentral heat pump systems supply space heat and domestic hot water to both buildings of building type 1. Innovative heat pump technologies are employed. The first heat pump system couples a high-temperature heat pump with refrigerant R134a to photovoltaic-thermal PVT collectors as single heat source. Simulations predict a performance comparable to the studied air source heat pump. The second heat pump system uses a combination of two heat sources: an outdoor air unit and an undersized borehole heat exchanger. Thus, investment costs are reduced while electricity consumption comparable to the studied ground source heat hump is expected.

In contrast to the simulation case in section 3, both heat pump systems are carried out as a bivalent system with a gas boiler as backup heater instead of the simulated electrical heating rod. Eleven radiators are replaced in both buildings in conjunction with a hydronic balance of the space heating system. Thus, the heating system is designed to operate at nominal temperatures of 55°C/45°C.

The three buildings of building type 2 are less suitable for the application of heat pumps due to their lower capacity of installed radiators. These buildings are connected to a heating plant, with two gas engine cogeneration units and a peak load gas boiler, via a district heating network. All buildings in the district feature roof top PV panels. In combination with a micro grid and a smart energy management system, the electricity for the heat pumps is predominantly supplied by locally generated PV modules and cogeneration units [31].

The district energy system is subject to an ongoing demonstration and monitoring project. In addition to the evaluation of the energy balance of the district and the performance of the heat pump systems also thermal comfort and occupant acceptance of

the buildings with reduced heating temperatures will be analyzed.

7. Conclusion

Low heating temperatures are essential for an energy and cost-efficient operation of heat pumps. Radiator heat emission systems in existing buildings are, however, typically designed for conventional heating systems with high temperatures. To analyze the viability of retrofitting heat pumps in buildings with radiator systems, this paper links the experimental and simulated performance analysis of heat pump systems with methods to reduce heating temperatures.

The mean heat pump temperature $T_{m,HP}$ is proposed as new indicator to describe the mean temperature level of heat pump operation over a heating period. Field data of 34 air source and 15 ground source heat pumps in retrofit buildings show an approximately linear correlation of the mean heat pump temperature and the seasonal performance factor. On average, every Kelvin of reduced heat pump temperature $T_{m,HP}$ increases the SPF_3 by 0.13 points (air source heat pump) and by 0.10 points (ground source heat pump). By means of detailed simulation of heat pump systems, the influence of heating temperatures on system performance is studied. These experimental and numerical findings quantify the effect of varying heating temperatures thus provide a systematic method to assess the seasonal performance factor SPF_3 via the mean heat pump temperature $T_{m,HP}$.

Applied methods to reduce heating temperatures are discussed at the example of two multi-family buildings. Thermally insulating the building envelope leads to reduced heat loads. As a result, the installed radiators allow a reduction of heating circuit temperatures. As single radiators limit a further reduction of heating temperatures, there is a significant potential to identify and exchange these critical radiators by analyzing the required heat load and installed radiator capacity per room. In one building type, the selective exchange of only 7 % of all radiators is sufficient to increase the radiator capacity so that nominal heating temperatures can be reduced from 75°C/60°C to 55°C/45°C. This corresponds to a reduction of the electricity consumption by 40 % (air source heat pump) and 42 % (ground source heat pump). However, a second building within the same district requires an exchange of 52 % of radiators to achieve the same temperature reduction. These findings are therefore specific to each individual building, depending particularly on its renovation state and the heat transfer capacity of installed radiators. Nonetheless, the selective radiator exchange is a measure with a large potential to improve energy-efficiency of heat pump systems in existing radiator systems, which can reduce heating costs of up to 24%.

There is a future need for research on heat pumps in radiator heat emission systems: advanced control approaches may adapt heating system temperatures dynamically to further optimize the system performance. Digital methods for automatized analysis of the building and its heating system may facilitate the design and planning of the heating systems. This also includes new methods for automatized and optimized hydronic balancing. Furthermore, heat pumps with adapted refrigerant circuits are a promising technology for existing buildings with higher temperature requirements. Finally, new technologies and approaches for energy-efficient and hygienic domestic water heating also need to be developed and validated.

In conclusion, an energy-efficient operation of heat pumps in existing buildings with radiators is viable, if following an integrated system design approach where the characteristics of the individual building, the heat emission system and the heat pumps are considered. The presented approach links heat pump performance with retrofit measures and thus allows the evaluation of performance improvements against retrofit measures to identify optimal solutions for any existing building.

Acknowledgement

We gratefully acknowledge financial support of the German Federal Ministry for Economic Affairs and Energy (BMWi) due to an enactment of the German Bundestag under grant numbers 03ET1590 (Smartes Quartier KA-Durlach), 03ET1272 (WPsmart im Bestand), and 03SBE0001 (LowEx-Bestand). We would like to thank all project partners for the fruitful cooperation and specially Dennis Hahn from IBS Ingenieurgesellschaft mbH for carrying out the heat load calculation per room.

Nomenclature

Symbols

A	area, m²
COP	coefficient of performance, -
E	electricity, kWh
$\dot{m}$	mass flow rate, kg s^{-1}
n	radiator exponent, -
P	electrical power, W
$\dot{Q}$	thermal power, W
Q	heat, kWh
T	temperature, °C
ΔT	temperature difference, K
SPF	seasonal performance factor, -

Abbreviations

AEC	annual energy costs
ANI	annuity of investment
ASHP	air source heat pump
GSHP	ground source heat pump

Subscripts

air	outdoor air
BU	backup unit
el	electrical
HP	heat pump
lim	heating limit
log	logarithmic
m	mean
nom	nominal, design
rad	raditator
rel	relative
ret	return
SH	space heating
SRC	environmental heat source
sup	supply
win	windows

8. References

[1] O. Lucon, D. Ürge-Vorsatz, Buildings. In: Climate Change 2014: Mitigation of Climate Change. Contribution of Working Group III to the Fifth Assessment Report of the Intergovernmental Panel on Climate Change [Edenhofer, O., R. Pichs-Madruga, Y. Sokona, E. Farahani, S. Kadner, K. Seyboth, A. Adler, I. Baum, S. Brunner, P. Eickemeier, B. Kriemann, J. Savolainen, S. Schlömer, C. von Stechow, T. Zwickel and J.C. Minx (eds.)]., Cambridge University Press, Cambridge, United Kingdom and New York, NY, USA., 2014.

[2] P. Sterchele, J. Brandes, J. Heilig, D. Wrede, C. Kost, T. Schlegl, Paths to a Climate-Neutral Energy System - The German Energy Transition in its Social Context, Fraunhofer Institute for Solar Energy Systems ISE, Freiburg (2020).

[3] A. David, B.V. Mathiesen, H. Averfalk, S. Werner, H. Lund, Heat Roadmap Europe: Large-Scale Electric Heat Pumps in District Heating Systems, Energies 10 (2017) 578. https://doi.org/10.3390/en10040578.

[4] D. Connolly, H. Lund, B.V. Mathiesen, S. Werner, B. Möller, U. Persson, T. Boermans, D. Trier, P.A. Østergaard, S. Nielsen, Heat Roadmap Europe: Combining district heating with heat savings to decarbonise the EU energy system, Energy Policy 65 (2014) 475–489. https://doi.org/10.1016/j.enpol.2013.10.035.

[5] G. Eggen, G. Breembroek, Retrofittung with heat pumps in buildings: Survey Report HPC - AR9, IEA Heat Pump Centre, Sittard, the Nethderlands (2001).

[6] M. Miara, D. Günther, R. Langner, S. Helmling, J. Wapler, 10 years of heat pumps monitoring in Germany. Outcomes of several monitoring campaigns. From low-energy houses to un-retrofitted single-family dwellings., 12th IEA Heat Pump Conference 2017 K.1.5.1 (2017).

[7] K. Huchtemann, D. Müller, Evaluation of a field test with retrofit heat pumps, Building and Environment 53 (2012) 100–106. https://doi.org/10.1016/j.buildenv.2012.01.013.

[8] P. Ovchinnikov, A. Borodiņecs, K. Strelets, Utilization potential of low temperature hydronic space heating systems: A comparative review, Building and Environment 112 (2017) 88–98. https://doi.org/10.1016/j.buildenv.2016.11.029.

[9] M. Jangsten, J. Kensby, J.-O. Dalenbäck, A. Trüschel, Survey of radiator temperatures in buildings supplied by district heating, Energy 137 (2017) 292–301. https://doi.org/10.1016/j.energy.2017.07.017.

[10] P. Lauenburg, J. Wollerstrand, Adaptive control of radiator systems for a lowest possible district heating return temperature, Energy and Buildings 72 (2014) 132–140. https://doi.org/10.1016/j.enbuild.2013.12.011.

[11] D.S. Østergaard, S. Svendsen, Replacing critical radiators to increase the potential to use low-temperature district heating – A case study of 4 Danish single-family houses from the 1930s, Energy 110 (2016) 75–84. https://doi.org/10.1016/j.energy.2016.03.140.

[12] A. Hasan, J. Kurnitski, K. Jokiranta, A combined low temperature water heating system consisting of radiators and floor heating, Energy and Buildings 41 (2009) 470–479. https://doi.org/10.1016/j.enbuild.2008.11.016.

[13] I. Sarbu, C. Sebarchievici, A study of the performances of low-temperature heating systems, Energy Efficiency 8 (2015) 609–627. https://doi.org/10.1007/s12053-014-9312-4.

[14] M. Maivel, J. Kurnitski, Heating system return temperature effect on heat pump performance, Energy and Buildings 94 (2015) 71–79. https://doi.org/10.1016/j.enbuild.2015.02.048.

[15] M. Maivel, J. Kurnitski, Low temperature radiator heating distribution and emission efficiency in residential buildings, Energy and Buildings 69 (2014) 224–236. https://doi.org/10.1016/j.enbuild.2013.10.030.

[16] Q. Wang, A. Ploskić, X. Song, S. Holmberg, Ventilation heat recovery jointed low-temperature heating in retrofitting—An investigation of energy conservation, environmental impacts and indoor air quality in Swedish multifamily houses, Energy and Buildings 121 (2016) 250–264. https://doi.org/10.1016/j.enbuild.2016.02.050.

[17] C. Fraga, P. Hollmuller, S. Schneider, B. Lachal, Heat pump systems for multifamily buildings: Potential and constraints of several heat sources for diverse building demands, Applied Energy 225 (2018) 1033–1053. https://doi.org/10.1016/j.apenergy.2018.05.004.
[18] A. Heinz, R. Rieberer, Energetic and economic analysis of a PV-assisted air-to-water heat pump system for renovated residential buildings with high-temperature heat emission system, Applied Energy 293 (2021) 116953. https://doi.org/10.1016/j.apenergy.2021.116953.
[19] Z. Nagy, D. Rossi, C. Hersberger, S.D. Irigoyen, C. Miller, A. Schlueter, Balancing envelope and heating system parameters for zero emissions retrofit using building sensor data, Applied Energy 131 (2014) 56–66. https://doi.org/10.1016/j.apenergy.2014.06.024.
[20] N. Calame, A. Freyre, F. Rognon, S. Callegari, M. Rüetschi, Air to water heat pumps for heating system retrofit in urban areas: understanding the multi-faceted challenge, J. Phys.: Conf. Ser. 1343 (2019) 12079. https://doi.org/10.1088/1742-6596/1343/1/012079.
[21] A. Ionesi, M. Jradi, J.E. Thorsen, C.T. Veje, Simulation of an adaptive heat curve for automatic optimization of district heating installation, Proceedings of BS2015: 14th Conference of International Building Performance Simulation Association, Hyderabad, India, Dec. 7-9, 2015. (2015).
[22] K. Huchtemann, D. Müller, Simulation study on supply temperature optimization in domestic heat pump systems, Building and Environment 59 (2013) 327–335. https://doi.org/10.1016/j.buildenv.2012.08.030.
[23] M. Tunzi, D.S. Østergaard, S. Svendsen, R. Boukhanouf, E. Cooper, Method to investigate and plan the application of low temperature district heating to existing hydraulic radiator systems in existing buildings, Energy 113 (2016) 413–421. https://doi.org/10.1016/j.energy.2016.07.033.
[24] DIN EN, DIN EN 14511: Luftkonditionierer, Flüssigkeitskühlsätze und Wärmepumpen mit elektrisch angetriebenen Verdichtern für die Raumheizung und-kühlung, DIN Deutsches Institut für Normung e. V. (2013).
[25] ASHRAE, ASHRAE handbook - Heating, ventilating, and air-conditioning applications, SI ed., ASHRAE, Atlanta, Ga., 2012.
[26] DIN, DIN 4703-3:2000-10- Raumheizkörper - Teil 3: Umrechung der Norm-Wärmeleistung: Heat appliances - part 3: conversion of the standard thermal output, DIN Deutsches Institut für Normung e. V. (2000).
[27] K.-J. Albers (Ed.), Recknagel - Taschenbuch für Heizung und Klimatechnik, 79th ed., ITM InnoTech Medien GmbH, Augsburg, 2018.
[28] M. Wetter, W. Zuo, T.S. Nouidui, X. Pang, Modelica Buildings library, Journal of Building Performance Simulation 7 (2014) 253–270. https://doi.org/10.1080/19401493.2013.765506.
[29] D. Günther, J. Wapler, R. Lagner, S. Helmling, M. Miara, Wärmepumpen in Bestandsgebäuden: Ergebnisse aus dem Forschungsprojekt "WPsmart im Bestand", Fraunhofer ISE (2020).
[30] A. Zottl, R. Nordmann, M. Coevoet, P. Riviere, M. Miara, A. Benou, P. Riederer, Sepemo Report D4.2. /D 2.4. - Concept for evaluation of SPF Version 2.2: A defined methodology for calculation of the seasonal performance factor and a definition which devices of the system have to be included in this calculation. Heat pumps with hydronic heating systems (2012).
[31] M. Lämmle, S. Hess, S. Herkel, Smart urban energy concept: integration of heat pumps, PV, cogeneration, and district heating in existing multi-family buildings, Eurosun 2020, ISES Conference Proceedings (2020). https://doi.org/10.18086/eurosun.2020.02.04.
[32] International Organization for Standardization, EN ISO 13790: Energy Performance of Buildings: Calculation of Energy Use for Space Heating and Cooling (ISO 13790: 2008), CEN, 2008.
[33] R. Jank, M. Lämmle, S. Hess, M. Kropp, Smartes Quartier Karlsruhe-Durlach (SQ-Durlach), Projektbericht Phase A: Konzeptentwicklung EnEff:Stadt - FKZ 03ET1590 (2020).
[34] D. Müller, M. Lauster, A. Constantin, M. Fuchs, P. Remmen, AixLib - An Open-Source Modelica Library within the IEA-EBC ANNEX 60 Framework: AixLib - An Open-Source Modelica Library within the IEA-EBC Annex 60 Framework. BauSIM 2016, p.3–9, September 2016. link, BauSIM (2016) 3–9.
[35] IBPSA, Modelica IBPSA library v 3.0, 2018. https://github.com/ibpsa/modelica-ibpsa.
[36] EN, EN 12831-1:2017 - Energy performance of buildings - Method for calculation of the design heat load - Part 1: Space heating load, European norm (2017).
[37] K. Jagnow, C. Halper, T. Timm, Optimization of heating plants in buildings. Pt. 1-5. Optimierung von Heizungsanlagen im Gebaeudebestand. Teil 1-5, TGA Fachplaner 2, 2003.
[38] C. Kost, S. Shammugam, V. Jülch, H.-T. Nguyen, T. Schlegl, Levelized Cost of Electricity- Renewable Energy Technologies: March 2018, Fraunhofer Institute for Solar Energy Systems ISE (2018).

Appendix – Sorted heat pump temperatures at varying heating temperatures

The mean heat pump temperature $T_{m,HP}$ describes the energy weighted temperature of the heat pump condenser averaged over an entire year. Fig. 13 gives a more profound insight into the occurrence of condenser temperatures $T_{HP} = (T_{HP,sup} + T_{HP,ret})/2$ with varying heating temperatures. This graph plots the sorted hourly temperatures in ascending order over their cumulated supplied heat $Q_{HP,}$ allowing a qualitative comparison of the condenser temperatures of the heat pump. Simulation results of the air source heat pump system in section 3.3 are evaluated for that purpose.
At nominal temperature of 55°C/45°C, for example, T_{HP} varies between 26.8 °C and 49.0 °C with a relatively homogenous distribution of temperatures. Within the temperature range of the heat pump, an increase or decrease of the nominal heating temperatures yields an approximately parallel shift of the temperature duration curve. Starting at 65°C/50°C, the supplied heat

Q_{HP} is reduced as the heat pump power drops at elevated supply temperatures. Moreover, the maximum condenser temperature of the heat pump of $T_{cond,max}$ = 60 °C is reached. As a result, the heat pump systems with nominal heating temperatures above 75°C/60°C have a frequent occurrence of the maximum operating temperature.

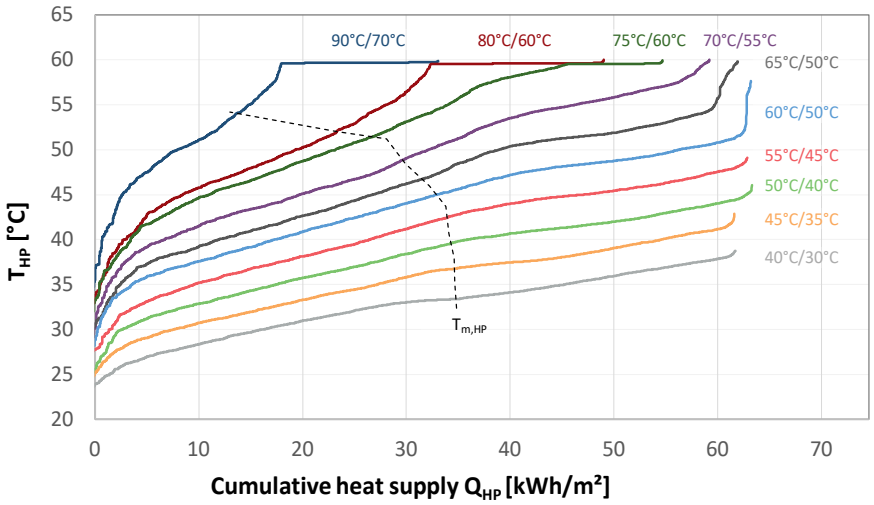

Fig. 13: Sorted condenser temperatures T_{HP} of the air source heat pump at varying heating temperatures.